Article

Understanding the Role of Electrolyte Cations on Activity and Product Selectivity of CO_2 Reduction over Cu Electrode

Aamir Hassan Shah [1,2], Yue Gong [1,2], Yanjie Wang [1,*], Abebe Reda Woldu [1,2] and Tao He [1,2,*]

1   CAS Key Laboratory of Nanosystem and Hierarchical Fabrication, National Center for Nanoscience and Technology, Beijing 100190, China
2   University of Chinese Academy of Sciences, Beijing 100049, China
*   Correspondence: wangyanjie@nanoctr.cn (Y.W.); het@nanoctr.cn (T.H.)

Abstract: The electrocatalytic conversion of CO_2 on a Cu electrode has the potential to produce valuable chemicals such as hydrocarbons and oxygenated compounds. While the influence of electrolyte cation on the activity and selectivity of the CO_2 reduction reaction (CO_2RR) on Cu has been widely observed, the specific mechanism through which cation species affect the CO_2RR remains unclear and subject to debate. In this work, the CO_2RR in the carbonate electrolytes containing different alkali metals (Li^+, Na^+, K^+, Rb^+, and Cs^+) was investigated at potentials from -0.1 to -1.1 V (vs. RHE) over a Cu electrode using electrochemical techniques. Charge transfer kinetics, adsorption of species, and mass transport were considered comprehensively during the analysis. It is found that several factors can play a role in the CO_2RR, including hydrated cation adsorption, preferential hydrolysis, and interaction between the cation and adsorbed species, with the dominating factor determined by the external bias and cation species. Consequently, a coherent interpretation of the influence of electrolyte cations on the intrinsic kinetics of the CO_2RR has been put forward. We envision that these insights will greatly contribute to the development of efficient catalytic systems and the optimization of catalytic conditions, thereby advancing progress toward commercial applications in this field.

Keywords: CO_2 reduction; electrolyte cations; Cu electrode; linear scan voltammetry; electrochemical impedance spectroscopy

1. Introduction

The electrocatalytic CO_2 reduction reaction (CO_2RR) offers an important strategy to store electrical energy produced via renewable and intermittent resources like wind, hydro, and solar energy [1–3]. The high energy density of hydrocarbons and alcohols make these products more preferable compared to carbon monoxide and formic acid. So far, extensive efforts have been invested to seek out such catalysts that can directly produce hydrocarbons or alcohols, but only copper (Cu) is known to catalyze the C-C coupling with appreciable efficiency to generate a wide range of multicarbon products in an aqueous solution [4–6]. However, the application of CO_2RR technology on a global scale faces significant technical challenges, including poor product selectivity, high overpotential, and slow reaction kinetics associated with Cu [7]. Consequently, gaining a comprehensive understanding of the reaction processes occurring on the surface of Cu is essential for the production of hydrocarbons and the precise tuning of target products [8]. The activity and selectivity of the CO_2RR are largely influenced by factors such as catalyst structure, electrolyte composition, and pH levels during the reaction [9–16]. In order to comprehend and manipulate these influences, state-of-the-art strategies should be employed.

A number of reports have indicated that the species of electrolyte cations can play a significant role in influencing the activity and product selectivity of the CO_2RR [2,17–25]. In the case of Cu electrodes, increasing the size of electrolyte alkali metal cations leads to

higher C2 selectivity, like for ethylene and ethanol [18,19,23]. However, the origination of the effects from electrolyte cations is intricate and is still contentious today. Previous reports revealed that these cations can be adsorbed on the electrode surface at the outer Helmholtz plane (OHP), giving rise to changes in the local electric property to different extents due to hydration and/or influence on the formation/stabilization of the reduction intermediates [2,22,26,27]; while other research suggests that the surface pH can be influenced by different sized cations owing to the discrepancy in their buffer capacity, thus changing the pH-dependent reaction routes or surface CO_2 concentration for the CO_2RR [19,28,29]. The consistent explanation of how the electrolyte cations influence the CO_2RR kinetics is challenging since the relevant factors in the electrolyte are complex (including mass transport, conductivity, and pH). Neglecting the comprehensive consideration of these factors can lead to confusion. For instance, Singh et al. have shown that cation-dependent pH at the electrode surface accounts for the different CO_2RR performances under inadequate mass transfer conditions [19]. On the other hand, Resasco and coworkers reported that the interfacial dipole field dominates the cation-dependent CO_2RR under the condition where influence from mass transport is avoided [2]. Therefore, robust methodologies are required to elucidate the specific role of cations in the CO_2RR over Cu electrodes, taking into account various influencing factors.

Directly extracting information at the electrode/electrolyte interface during the reaction would be promising to study the influential mechanism of the electrolyte cations. According to classic catalytic theory, the properties of the electrode/electrolyte interface, such as the electrode/cation interaction, play a significant role in the reaction by regulating the local electrical field, charge, and mass transfer, as well as the adsorption/desorption process. However, the understanding of the electrode/cation interface remains limited primarily due to the lack of well-established characterization techniques for studying the electrolyte and its interaction with the electrode. Electrochemical characterization offers a mature and useful approach to comprehensively probe in an operando manner the electrode/electrolyte interface [30]. Linear scan voltammetry (LSV) and electrochemical impedance spectroscopy (EIS) are frequently used techniques to study the kinetics of electrode processes in the CO_2RR [31–35]. These methods are valuable as they can provide direct insights into the interfacial redox reaction mechanism at a low cost. Specifically, EIS enables the qualitative analysis of the kinetics of redox processes at the electrode/electrolyte interface, the adsorption/desorption behavior of species on the electrode surface, and mass transport. Recently, LSV and EIS were successfully applied to identify the processes during the CO_2RR on tin foil [36]. However, the utilization of electrochemical techniques in analyzing the effect of electrolyte cations is still lacking and requires further exploration.

Herein, we performed a systematic electrochemical study to elucidate the origination of the electrolyte cation effect in the CO_2RR over the Cu electrode. The information on charge transfer processes, adsorption of intermediates, and mass transport during the CO_2RR was analyzed in detail. While the cation effect on activity and selectivity of the CO_2RR have been reported previously [2,19], our work offers a more comprehensive approach by investigating the mechanism across a broad range of applied potentials. The role of cations with varying sizes and their influence on the CO_2RR under different potentials are thoroughly investigated.

2. Results and Discussion

It has been reported experimentally that the CO_2RR dominates over the hydrogen evolution reaction (HER) in electrolytes with larger cations (K^+, Rb^+, Cs^+) compared to the smaller ones (Li^+ and Na^+) [2,18,19]. Meanwhile, the driving force is an important factor regulating the CO_2RR performance [37]. Thus, the following discussion is divided into different parts, large (K^+, Rb^+, Cs^+) and small (Li^+ and Na^+) cations, and high (−0.6 to −1.1 V) and low (−0.1 to −0.5 V) negative applied bias voltages. In addition, it should be pointed out that here, the discussions are based on the previously reported product

distribution data affected by the electrolyte cations [2,19]. As the cation size becomes larger, HER is inhibited, and selective CO_2RRs (especially C2 production) are favored.

2.1. Linear Scan Voltammetry

To investigate the influence of electrolyte cations on the Faradic current over the Cu electrode, LSV was carried out in CO_2-saturated M_2CO_3 electrolytes (0.1 M, M = Li, Na, K, Rb, and Cs) (Figure 1). Figure 1a presents the LSV curves of the Cu electrode in CO_2-saturated Li_2CO_3 and Na_2CO_3 solutions. A higher cathodic current density and onset potential can be observed for the reaction in the Li_2CO_3 electrolyte in the low negative potential region due to the higher HER and more facile charge transfer kinetics as compared to that in the Na_2CO_3 electrolyte. Both the onset potential and the cathodic current density increase once the cation size further increases from K^+ to Cs^+ (Figure 1b), demonstrating a more facile catalytic reaction in the case of a larger cation size. The level of cation hydration and extent of cation adsorption can explain this phenomenon well. The larger cations possess lower hydration power, and much more can be adsorbed on the electrode surface in the outer Helmholtz plane (OHP) [22]. Generally, the potential at OHP can be elevated by the adsorbed cations, leading to decreased concentration of positive H^+ and accelerated the CO_2RR by stabilizing the negatively charged intermediate $CO_2 \cdot^-$, thereby suppressing HER and enhancing the CO_2RR. Therefore, for the reactions in electrolytes with large cations (K^+, Rb^+, Cs^+) where the CO_2RR dominates [18], the cathodic current density increases with the increase in cation size, as shown in Figure 1b. However, for the HER favorable cations in Figure 1a, since Na^+ has a higher propensity to be adsorbed on the electrode than Li^+, the repulsion of H^+ from OHP is more pronounced in the Na^+ electrolyte, resulting in lower current density than that in Li^+.
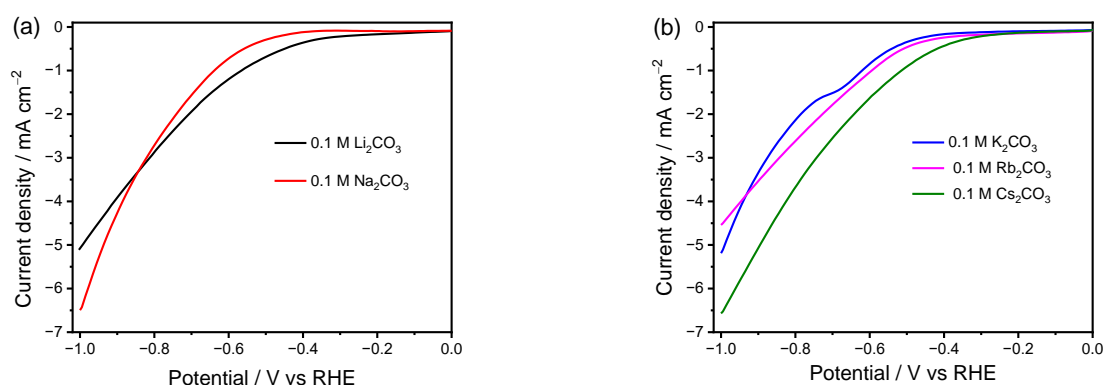

Figure 1. LSV curves of Cu electrode in 0.1 M CO_2-saturated electrolytes. (**a**) Li_2CO_3 and Na_2CO_3 and (**b**) K_2CO_3, Rb_2CO_3, and Cs_2CO_3. Scanning rate of 50 mV s^{-1}.

It is noted that the driving force starts to meet the requirement for the CO_2RR as the applied potential becomes more negative, like <-0.84 V (Figure 1a), which is more favorable to occur in the Na_2CO_3 electrolyte. A higher current density at more negative potentials in Na_2CO_3 than that in Li_2CO_3 indicates that other factors, rather than hydration discrepancy in the cations, become dominant in this region. According to previous reports, the CO_2RR is mass transport limited at high cathodic current [38,39]. The hydrated cations can act as a buffer to maintain the interfacial pH value. A larger cation tends to exhibit higher power to sustain a low local pH near the electrode, and thus keeps the concentration of local CO_2 at a higher level than that for a smaller cation [19,28,29]. Accordingly, the difference in buffer effect can reasonably explain the higher current density in Na_2CO_3 electrolyte than that in Li_2CO_3 under a more negative bias.

In addition, the current density in the K_2CO_3 solution exceeds that in Rb_2CO_3 at more negative potentials (Figure 1b). A hump in the LSV curve can be observed in K_2CO_3 at around -0.65 V, which is probably due to the reduction of CO_2 to CO. However, this hump cannot be observed in any other electrolytes. Such abnormal phenomena indicate that

other factors caused by the cation also play a role in the CO_2RR. It is widely accepted that the catalytic performance of the CO_2RR and HER can be impacted by various processes, such as mass transfer, adsorption/desorption of species, and local pH. The EIS analysis is thus carried out to further investigate the influential mechanism of cations on the catalytic performance over Cu electrodes under different applied biases.

2.2. Electrochemical Impedance Spectroscopy

EIS is a powerful tool to probe the information at the electrode/electrolyte interface. Charge transfer kinetics and mass transport can be deduced from the EIS plot. In addition, the behavior of capacitance and inductance of an electrode process influences not only the magnitude of alternating current in the impedance spectroscopy, but also the phase, which can help analyze the adsorption/desorption phenomena. A negative value of the phase angle is usually ascribed to the adsorption of chemical species. The peak in the phase angle plot corresponds to the time constant, i.e., the charge transfer process at the electrode/electrolyte interface. Therefore, both the impedance and phase are taken into consideration in the following EIS analysis so as to study the electrochemical behavior at the electrode/electrolyte interface. The EIS was performed in a CO_2-saturated 0.1 M M_2CO_3 electrolyte under different applied bias voltages. As analyzed in Figure 1, the Faradic reaction over the Cu electrode strongly depends on the cation size and applied potential. To clearly interpret the process, the impedance behavior of the Cu electrode in solutions with small (Li^+ and Na^+) and large cations (K^+, Rb^+, and Cs^+) were studied and explained separately. For each of them, two different potential ranges, i.e., less (-0.1 to -0.5 V) and more (-0.6 to -1.1 V) negative potentials, were employed to study the process at the electrode/electrolyte interface during the electrolysis. Three different equivalent circuits are used to interpret the EIS spectra depending on the elements in the data, $R_s(R_{ct}CPE)$, $R_s((R_{ct}Z_W)CPE)$, and $R_s((R_{ct}Z_W)CPE_1)((R_lL)R_{ct}CPE_2))$, where R_s represents series resistance; the constant phase elements CPE, CPE_1, and CPE_2 represent the capacitance; R_{ct} and R_l are the charge transfer resistance; Z_W is the Warburg impedance that describes diffusion process; and the inductive impedance L represents the adsorption process.

2.2.1. EIS Plots of Cu Electrode in Li_2CO_3 and Na_2CO_3 Electrolyte

The spectra recorded at less negative potentials are presented as Nyquist (Figure 2a) and Bode plots (Figure 2b,c), respectively. The impedance modulus has almost the same value for the two systems at a high frequency that corresponds to $\theta = 0$ in the phase angle plots, which is the solution resistance between working and reference electrodes. The difference in ionic conductivity of the electrolytes with different cations is thus not considered in this work. It is noted that in most cases, only one characteristic peak is observed in Bode plots due to the charge transfer process (Figure 2c). The charge transfer resistance (R_{CT}) is directly proportional to the arc radius in the Nyquist plot (Figure 2a), which decreases as the applied potential becomes more negative due to faster charge kinetics upon a larger driving force. Lower R_{CT} in Li_2CO_3 than in Na_2CO_3 is observed at the same potential, indicating a more facile charge transfer at the Cu/electrolyte interface in Li_2CO_3.

The spectra in Figure 2a can reflect the HER to some degree during the electrolysis in Li_2CO_3 under low applied bias. In comparison, a different character in the Nyquist plot is observed for the Na_2CO_3 electrolyte, with an inductive loop in the low-frequency region. It is speculated that this is due to the adsorption process of the CO_2RR intermediate and/or CO_2. Specifically, since the ability to initiate the CO_2RR is stronger in Na_2CO_3 than in Li_2CO_3 and a low overpotential is not large enough to drive efficient CO_2RR and consume the adsorbates, reactants are easier to be adsorbed and/or accumulated on the Cu surface in Na_2CO_3, manifested as an inductive loop in the Nyquist plot (Figure 2a). It is worth mentioning that the adsorbates can block the active sites on the Cu electrode surface and can thus decrease the current density [40]. Hence, in addition to the more facile HER in Li_2CO_3 as compared to that in Na_2CO_3, the greater adsorption extent in Na_2CO_3 can also

suitably explain the lower current density in LSV at a less negative potential (Figure 1a) and higher R_{CT} (Figure 2a) in Na_2CO_3 as compared to in Li_2CO_3.
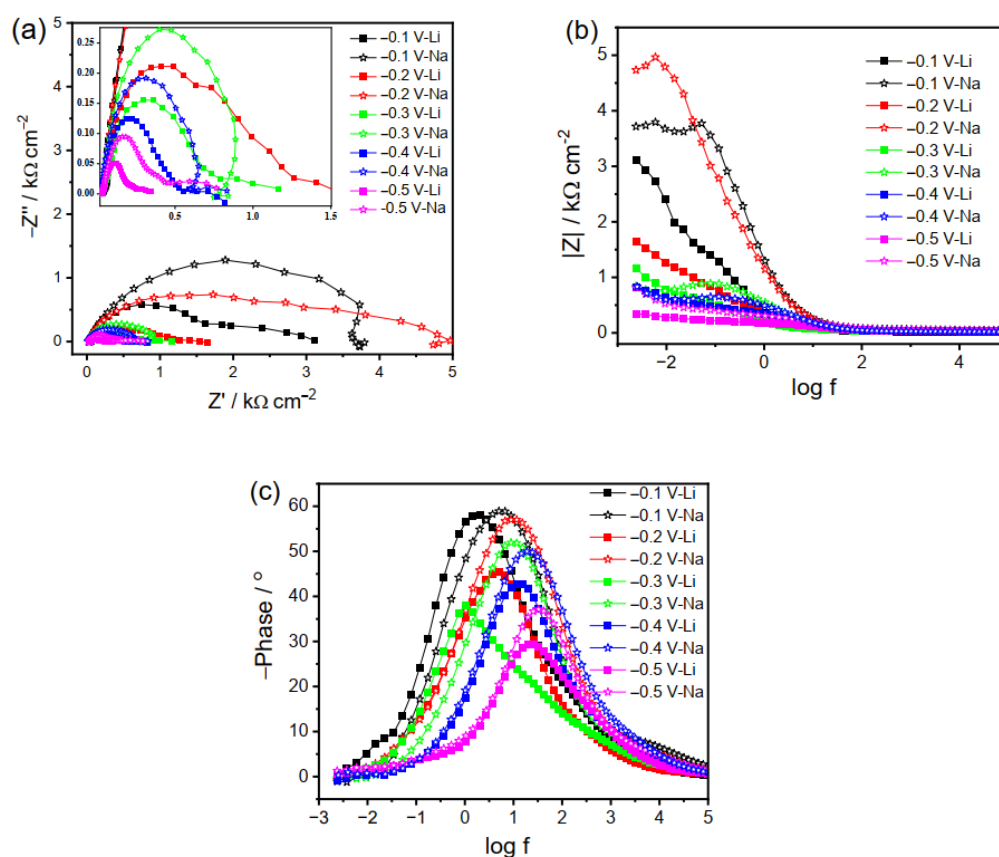

Figure 2. EIS spectra of Cu electrode in CO_2-saturated 0.1 M Li_2CO_3 and Na_2CO_3 under less negative bias voltages (-0.1 to -0.5 V). (**a**) Nyquist plots and corresponding Bode plots of (**b**) impedance vs. frequency and (**c**) phase vs. frequency. Inset is zoom-in of the figure.

Interestingly, a sharp decrease in R_{CT} is observed at -0.3 V in the Na_2CO_3 electrolyte as compared to those at -0.1 and -0.2 V (Figure 2a,b), implying that -0.3 V is the critical potential for the beginning of the Faradic reaction. Likewise, a further decrease in the applied potential (such as -0.4 V) can result in further decrement in the R_{CT} value. Thus, the EIS results further prove that in the less negative potential region, reactions proceed easier in Li_2CO_3 than in Na_2CO_3 due to the dominant HER and less blockage of the Cu surface by the adsorbates.

As the applied potential becomes more negative (i.e., -0.6 to -1.1 V), a reversal in the R_{CT} occurs, i.e., faster charge transfer kinetics at the electrode/electrolyte interface in Na_2CO_3 as compared to Li_2CO_3 (Figure 3). This reversal suggests more facile charge transfer in the Na_2CO_3 electrolyte, as the high potential can drive charge transfer to the adsorbed species, which will otherwise passivate the electrode surface and hinder the reduction reactions at less negative potentials. Interestingly, only one arc is observed in the Nyquist plots at high frequency (Figure 3a), perhaps because of the comparable or merged time constants of different reactions. Since various products can be produced during the CO_2RR via sequential reduction reactions along with HER, the apparent single time constant is indeed a combination of several time constants [36]. Similarly, the negative phase angle values at low frequency imply the intermediate's adsorption under high applied potential.
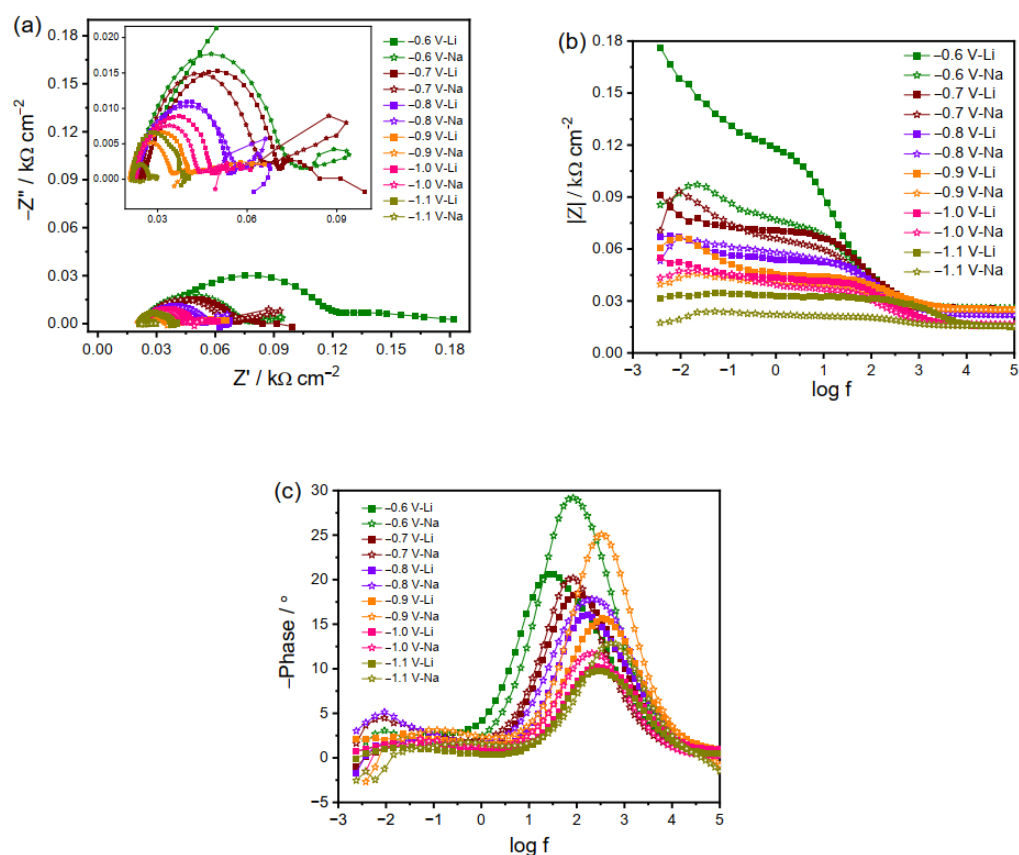
Figure 3. EIS spectra of Cu electrode in CO_2-saturated 0.1 M Li_2CO_3 and Na_2CO_3 under more negative bias voltage (-0.6 to -1.1 V). (**a**) Nyquist plots and corresponding Bode plots of (**b**) impedance vs. frequency and (**c**) phase vs. frequency. Inset is zoom-in of the figure.

An exception is that a charge transfer process without an inductive element is observed at a low frequency for the reaction in Li_2CO_3 at -0.6 V, which may be caused by the low amount of adsorbates that can be consumed instantly. As the applied potential becomes more negative, the impedance spectra in Li_2CO_3 electrolyte start to resemble those in Na_2CO_3 with diffusion and adsorption process observed, as a higher driving force can lead to faster charge kinetics and thus a high amount of adsorbed CO_2RR intermediates and/or exhausted molecular CO_2 at the electrode surface and, thereby, the rate-determining step of CO_2 diffusion.

It is worth mentioning that the low-frequency arc representing the diffusion process can be observed at high applied potentials (Figure 3a), indicating the accelerated reactions due to rapid consumption of CO_2, which is more prominent for those in Na_2CO_3. It is noted that the surface pH rises during the catalytic reaction, resulting in a pH gradient in the vicinity of the electrode [41,42]. The pH value adjacent to the electrode is high at large negative applied potential due to the weak buffer capacity of Li^+ and Na^+. As the CO_2 solubility is pH dependent, the concentration of surface molecular CO_2 decreases as the local pH becomes higher. Thus, dissolved molecular CO_2 will transport to the electrode surface for equilibrium and supplement. Considering CO_2 is consumed in a faster way in the electrolyte containing larger Na^+ cations, the diffusion element can be observed in a clearer way in the Na_2CO_3 electrolyte than in Li_2CO_3.

2.2.2. EIS Plots of Cu Electrode in K_2CO_3, Rb_2CO_3 and Cs_2CO_3 Electrolyte

The EIS plots of Cu electrode in the electrolytes with larger cations (K^+, Rb^+, and Cs^+) behave differently than those with smaller ones (Li^+ and Na^+), as the larger cations adsorbed on the electrode surface can influence the interfacial reactions in more complicated

ways as compared to the smaller ones. The R_{CT} at less negative potentials decreases in the following order: $K^+ < Rb^+ < Cs^+$ (Figure 4a,b). At -0.1 V in the K_2CO_3 electrolyte, the inductive loop at low frequency shows adsorption behavior on the Cu electrode, as evidenced by the negative phase in Figure 4c, which is otherwise absent in the case of the Rb_2CO_3 and Cs_2CO_3 electrolytes. Such difference at -0.1 V is probably due to the neutral or positive property of the adsorbed species and greater blockage extent of the electrode surface by Rb^+ and Cs^+ as compared to K^+. The sharp decrease in impedance at -0.3 V additionally supports the above conclusion that it is the critical CO_2RR potential that is similar to that in the Na_2CO_3 electrolyte. Further reducing the applied potential will decrease the impedance and facilitate the CO_2RR. Reactions at the potentials of -0.4 and -0.5 V give rise to a new semicircle at low frequency, probably corresponding to the reduction of the intermediates.
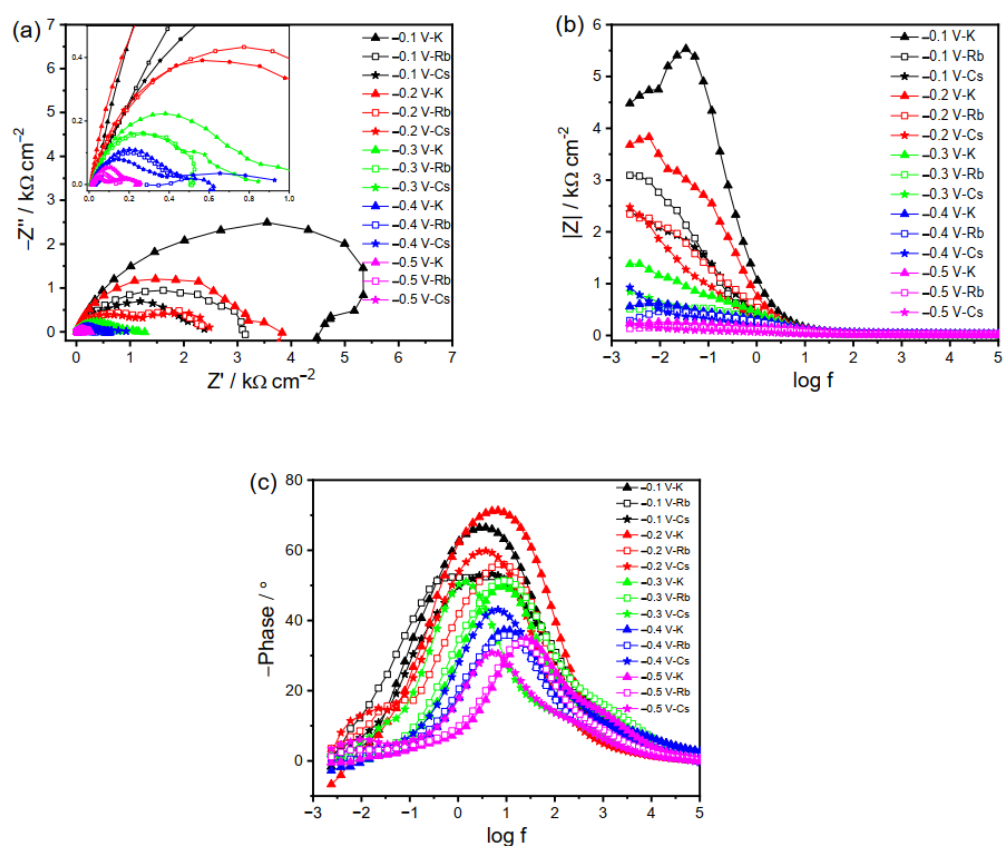

Figure 4. EIS spectra of Cu electrode in CO_2-saturated 0.1 M K_2CO_3, Rb_2CO_3, and Cs_2CO_3 at less negative bias voltage (-0.1 to -0.5 V). (**a**) Nyquist plots and corresponding Bode plots of (**b**) impedance vs. frequency and (**c**) phase vs. frequency. Inset is zoom-in of the figure.

For the reactions in Rb_2CO_3, the charge transfer is more facile as compared to that in K_2CO_3. Although it is hard to distinguish, it seems the EIS in Rb_2CO_3 at -0.1 V consists of two different time constants, as manifested by the two peaks in Figure 4c. It becomes more evident at potentials < -0.2 V, with a new semicircle appearing in the Nyquist plot, representing the sequential charge transfer processes. A small inductive loop at low frequency by further reducing the potential (-0.4 and -0.5 V) suggests the intermediates' adsorption. Likewise, the impedance plot for Cs_2CO_3 shows a similar phenomenon to that for Rb_2CO_3 at -0.1 V. However, the impedance spectra at -0.2 to -0.5 V for Cs^+ cation present two semicircles related to the charge transfer processes, with no inductive loop observed. This may be due to the fact that the adsorbed species can be consumed instantly, owing to the fast reaction kinetics in the Cs_2CO_3 electrolyte.

Figure 5 presents the impedance spectra at high negative potentials where the CO_2RR is dominant. At -0.6 V, the impedance behavior is similar in the three electrolytes, i.e., two distinct peaks corresponding to two separate time constants. The decrease in impedance magnitude with increasing negative potential is again attributed to the faster kinetics under high negative biases. At potentials from -0.7 to -1.1 V, the charge transfer kinetics follows the order of $K^+ < Cs^+ < Rb^+$ (Figure 5). So far, it is still unclear why the EIS spectra exhibit an elevated charge transfer in the electrolyte with smaller-sized Rb^+ than Cs^+. A possible speculation is that not only the cation size but also the nature of products play a role in this potential region. It is reported that HER is more favored at -1 V in Rb_2CO_3 electrolytes than in the K_2CO_3 and Cs_2CO_3 electrolytes, demonstrating a lower reaction barrier in electrolytes containing Rb^+ [2]. Moreover, the inductive loop in the low-frequency region becomes evident in these three electrolytes (Figure 5), indicating the intermediates' adsorption on the electrode surface at a large driving force, which is otherwise absent under less negative bias. As manifested by the inductive loop, the greater adsorption extent for large cations shown in Figure 5 than that for the smaller ones presented in Figure 3 indicates that the large cations in the electrolyte can stabilize the intermediates on the electrode surface in a better way. These results imply that the adsorption phenomena on the electrode surface depend on the bias voltage and electrolyte cation size. Given the dynamic nature of the processes involved in the generation, stabilization, and reduction of intermediates, it is not universally valid that selective and efficient CO_2RRs come from the high extent of adsorption. Figure 5 indicates that the adsorption decreases in the case of large cations and at high negative potentials like reactions in Cs_2CO_3 at -1 V, probably due to the rapid consumption of negatively charged intermediates and, thus, efficient generation of the final products. Moreover, mass diffusion can also be observed in Figure 5, which is more prominent than that in small cation electrolytes shown in Figure 3.
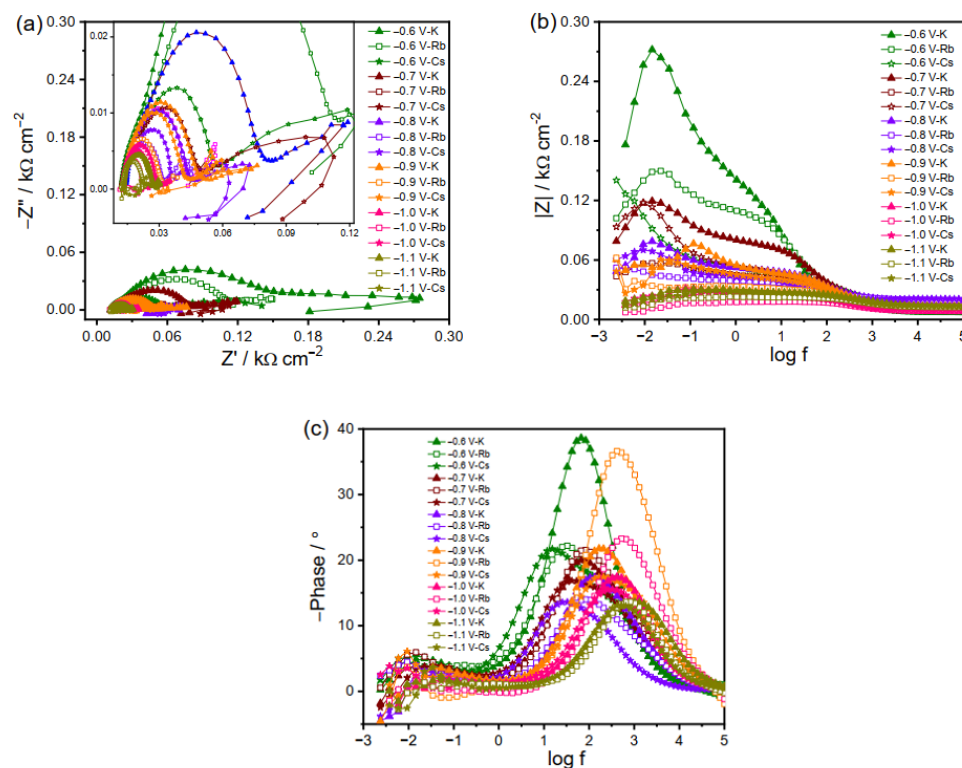

Figure 5. EIS spectra of Cu electrode in CO_2-saturated 0.1 M K_2CO_3, Rb_2CO_3, and Cs_2CO_3 under more negative bias voltages (-0.6 to -1.1 V). (**a**) Nyquist plots and corresponding Bode plots of (**b**) impedance vs. frequency and (**c**) phase vs. frequency. Inset is zoom-in of the figure.

2.3. Mechanism Analysis of Cations Effect on CO$_2$RR

Different theories have been proposed previously for the cation effect on the CO$_2$RR over the Cu electrode, including hydrated cation adsorption, preferential hydrolysis, and interaction between the cation and adsorbed species. However, there are still some phenomena that cannot be explained by these theories. For example, it was reported that higher local pH is favorable for the intermediates' dimerization and hence the formation of C2 products [43]. According to this claim, it is expected that the higher local pH in the case of small cations with less buffering capacity should produce more C2 products. However, the trend is the opposite, and the C2 formation is more favorable in the electrolyte with large cations [2]. Thus, not only do the buffering capacity and modulation of local pH account for the CO$_2$RR performance, but other factors can also play a part. On the basis of the LSV and EIS analysis here, it is found that the CO$_2$RR performance over the Cu electrode in electrolytes with different cations is a result of the interplay among various factors, including effects from the cation hydration, hydrolysis, and adsorption processes. The dominant factor influencing the electrochemical reactions is determined by both the cations and the applied potentials, and their specific influences are summarized in Figure 6.
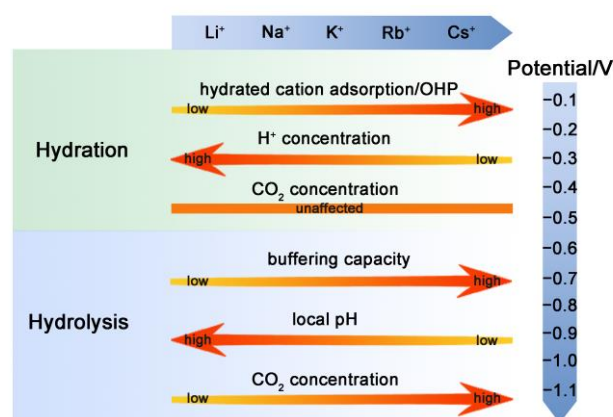

Figure 6. Effects of electrolyte cations on CO$_2$RR.

At low negative potentials, mass transport is not the rate-determining step for the CO$_2$RR, and variation in the local pH resulting from cation hydrolysis cannot be the major factor either since it is negligible, or no CO$_2$RR occurs under such conditions. The reaction in electrolytes with small cations (Li$^+$ and Na$^+$) and the dominant HER are taken as examples here to explain the influence of cation hydration. If the cations are strongly hydrated, it would be unfavorable for them to be adsorbed on the electrode. According to the literature [22], the hydration power is in the order of Li$^+$ > Na$^+$ > K$^+$ > Rb$^+$ > Cs$^+$. Therefore, the smaller cation with a higher hydration number, like Li$^+$, tends to adsorb less on the Cu electrode as compared to the larger ones [44], leading to a lower increase in the OHP potential with less blocked surface by the cations (Figure 6). The concentration of H$^+$ is inversely proportional to the value of OHP potential since it is positively charged, while the concentration of CO$_2$ is not influenced by OHP potential because it is not electrically charged (Figure 6). Thus, the cation hydration can impose a larger influence on the HER under low overpotentials. The cations adsorption and hydration propensity of small and large cations is schematically shown in Figure 7a,b, respectively. In the electrolyte with small cations and more negative OHP potential, the concentration of H$^+$ ions at the Cu electrode surface is higher than that of the large cations, according to Equation (1) [22]:

$$[\text{H}^+]_{\text{electrode}} = [\text{H}^+] exp^{\frac{-\text{F}\varphi}{\text{RT}}} \tag{1}$$

where [H$^+$]electrode and [H$^+$] are the respective H$^+$ concentration at the surface and in the bulk, F is Faraday's constant, φ is the OHP potential, R is the general gas constant, and T is the absolute temperature. The increase in [H$^+$]electrode leads to a higher HER and,

hence, faster charge transfer kinetics at the electrode surface, as manifested in the Nyquist plots (i.e., higher HER in Li^+ than in Na^+ in the potential range of -0.1 V to -0.5 V). These results agree well with the previously observed phenomenon of an increase in the HER with an increase in the electrolyte concentration due to the decrement in OHP potential [45].
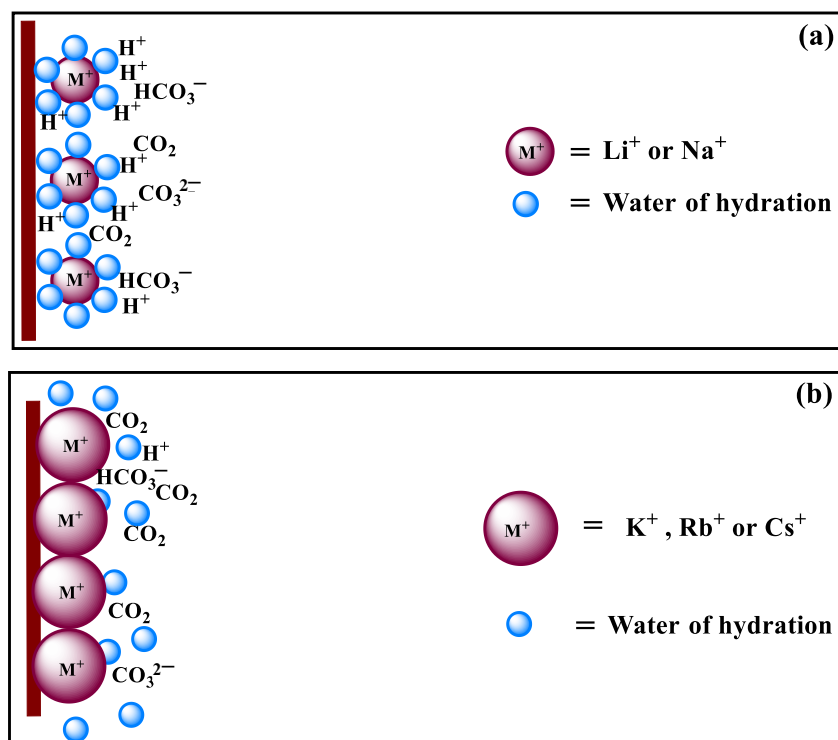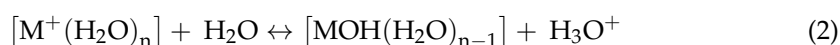

Figure 7. Illustration of cation hydration on the surface of Cu electrode during the CO_2RR in aqueous carbonate media: (**a**) small and (**b**) large alkali metallic cations.

At high negative potentials, CO_2 is consumed quickly, and a local pH gradient is built [46]. Thus, the hydrolysis of cations starts to take action, which can provide a buffering effect on the local pH (Figure 6). The reaction in electrolytes with large cations (K^+, Rb^+, and Cs^+) and dominant CO_2RRs are taken as an example. In general, the cations undergo hydrolysis by following Equation (2):

$$\left[M^+(H_2O)_n\right] + H_2O \leftrightarrow \left[MOH(H_2O)_{n-1}\right] + H_3O^+ \tag{2}$$

The distribution of dissolved CO_2 among molecular CO_2, HCO_3^-, and CO_3^{2-} is highly pH dependent, and a high pH value leads to reduced concentration of molecular CO_2 due to its rapid consumption with hydroxyl anions to form HCO_3^- and CO_3^{2-} at high negative potentials. A reduction in the pH near the cathode surface induced by the buffering action of large alkali metal cations can cause an increase in the concentration of dissolved molecular CO_2 at the electrode surface and, thereby, increase selective CO_2RR. Usually, a larger cation possesses a stronger buffering capacity (Figure 6). Among the three large cations, the Cs^+ ions are expected to give rise to minimal local pH, followed by Rb^+ and K^+. The low local pH can help to maintain the local CO_2 at a high level in the electrolyte with large cations than with small ones, favoring the selective CO_2RR and suppressing the HER from the aspect of CO_2 supply like Cs^+ (Figure 6). Another important factor worth mentioning is the ability to adsorb/stabilize the intermediates, as manifested by the EIS results. Cations play a significant role in the adsorption of CO_2 and other intermediates by changing their local concentration and stabilities. The interaction between cations and the species in solution can work through both the medium-range and short-range effects. For the medium-range effects (i.e., field-dipole interactions), the higher concentration of

larger cations at OHP can result in stronger electrostatic interaction between cations and the adsorbed intermediates having large dipole moments, and thereby enhance the CO_2RR compared to the smaller cations [2]. Moreover, a large cation can interact with more than one intermediate simultaneously, favoring the formation of C2 products [47]. For the short-range (i.e., electrostatic interactions), the stabilization of negatively charged CO_2RR intermediates can be strengthened by coordinating with partially dehydrated cations [48]. Thus, various effects played by the electrolyte cations balance in the case of different conditions, eventually leading to various CO_2RR performances in diverse electrolytes.

3. Materials and Methods

3.1. Materials

Various metal carbonates (99.999% metal basis) were purchased from Sigma-Aldrich (Shanghai, China). Copper (Cu) foil (99.9999% metal basis) was bought from Alfa Aesar (Shanghai, China). CO_2 ($\geq$99.999%) and argon (Ar, $\geq$99.9992%) were used to purge the electrolyte. Ultra high-purity water (18.2 MΩ cm) obtained from a Millipore system (Molsheim, France) was used through the experiments.

3.2. Electrode and Electrolyte Preparation

Cu foil (Figure S1) was cut into 1×1 cm^2 pieces, which were cleaned by sonication consecutively in acetone, isopropyl alcohol, and water for 30 min. Then, the Cu electrode was electro-polished at 2 V for 30 min in 85% phosphoric acid, followed by being rinsed with water and dried by Ar stream (Figure S2). Aqueous electrolyte of 0.1 M metal carbonate (M_2CO_3, M = Li, Na, K, Rb, and Cs) was prepared and purged with Ar for 30 min and CO_2 for another 60 min before the measurements.

3.3. Electrochemical Measurements

Electrochemical characterizations were carried out using an IM6 electrochemical workstation (Zahner, Kronach, Germany). Linear scan voltammetry (LSV) and electrochemical impedance spectroscopy (EIS) were performed with a homemade electrochemical cell, using Pt foil as the counter electrode and Ag/AgCl as the reference electrode (Figure S2). The potentials in this work were all converted to RHE scale by using the equation E(vs. RHE) = E(vs. Ag/AgCl) + 0.059pH +0.197. A slight negative potential was first applied to the electrode before all the electrochemical measurements so as to avoid the formation of oxides on the Cu surface. LSV was carried out from 0 to -1 V at a scanning rate of 50 mV s^{-1}. EIS spectra were collected in the frequency range of 1.5 mHz to 100 kHz in a potentiostatic mode with an AC amplitude of 100 mV. The applied bias in EIS was varied from -0.1 to -1.1 V in order to analyze the potential dependent electrocatalytic performance. The above experiments were repeated at least three times to ensure the results were reasonable and reproducible.

4. Conclusions

In summary, LSV and EIS were performed to probe the influence mechanism of different alkali metal cations in electrolytes on the CO_2RR over the Cu electrode. The results indicate that the influence of cations is not solely on the basis of their function from one aspect. Several factors, including hydrated cation adsorption, preferential hydrolysis, and interaction between the cation and adsorbed species, should be taken into account comprehensively. The dominant factor in the reaction varies with the external bias and cations. Specifically, at low negative potentials, the alteration of potential at OHP and interaction between the cations and adsorbed species in OHP have an impact on the performance, especially in the case of small cations like Li$^+$ and Na$^+$. When at high negative potentials, the influence of the difference in cation hydrolysis and surface adsorption dominates in the reaction, especially for the large cations of K$^+$, Rb$^+$, and Cs$^+$. Rational control of the delicate balance between these factors should lead to better regulation of the CO_2RR over the Cu electrode. We envision that this work will take a step forward in

understanding the role of cations in tuning the electrode/electrolyte interface and, thus, the activity and selectivity of the CO_2RR.

References

1. Lewis, N.S.; Nocera, D.G. Powering the planet: Chemical challenges in solar energy utilization. *Proc. Natl. Acad. Sci. USA* **2006**, *103*, 15729–15735. [CrossRef] [PubMed]
2. Resasco, J.; Chen, L.D.; Clark, E.; Tsai, C.; Hahn, C.; Jaramillo, T.F.; Chan, K.; Bell, A.T. Promoter effects of alkali metal cations on the electrochemical reduction of carbon dioxide. *J. Am. Chem. Soc.* **2017**, *139*, 11277–11287. [CrossRef] [PubMed]
3. Kang, Y.; Kim, T.; Jung, K.Y.; Park, K.T. Recent progress in electrocatalytic CO_2 reduction to pure formic acid using a solid-state electrolyte device. *Catalysts* **2023**, *13*, 955. [CrossRef]
4. Kuhl, K.P.; Hatsukade, T.; Cave, E.R.; Abram, D.N.; Kibsgaard, J.; Jaramillo, T.F. Electrocatalytic conversion of carbon dioxide to methane and methanol on transition metal surfaces. *J. Am. Chem. Soc.* **2014**, *136*, 14107–14113. [CrossRef] [PubMed]
5. Hori, Y.; Wakebe, H.; Tsukamoto, T.; Koga, O. Electrocatalytic process of CO selectivity in electrochemical reduction of CO_2 at metal electrodes in aqueous media. *Electrochim. Acta* **1994**, *39*, 1833–1839. [CrossRef]
6. Zarandi, R.F.; Rezaei, B.; Ghaziaskar, H.S.; Ensafi, A.A. Electrochemical reduction of CO_2 to ethanol using copper nanofoam electrode and 1-butyl-3-methyl-imidazolium bromide as the homogeneous co-catalyst. *J. Environ. Chem. Eng.* **2019**, *7*, 103141. [CrossRef]
7. Kuhl, K.P.; Cave, E.R.; Abram, D.N.; Jaramillo, T.F. New insights into the electrochemical reduction of carbon dioxide on metallic copper surfaces. *Energy Environ. Sci.* **2012**, *5*, 7050–7059. [CrossRef]
8. Sa, Y.J.; Lee, C.W.; Lee, S.Y.; Na, J.; Lee, U.; Hwang, Y.J. Catalyst-electrolyte interface chemistry for electrochemical CO_2 reduction. *Chem. Soc. Rev.* **2020**, *49*, 6632–6665. [CrossRef]
9. Hahn, C.; Hatsukade, T.; Kim, Y.G.; Vailionis, A.; Baricuatro, J.H.; Higgins, D.C.; Nitopi, S.A.; Soriaga, M.P.; Jaramillo, T.F. Engineering Cu surfaces for the electrocatalytic conversion of CO_2: Controlling selectivity toward oxygenates and hydrocarbons. *Proc. Natl. Acad. Sci. USA* **2017**, *114*, 5918–5923. [CrossRef]
10. Feng, X.; Jiang, K.; Fan, S.; Kanan, M.W. A direct grain-boundary-activity Correlation for CO electroreduction on Cu nanoparticles. *ACS Cent. Sci.* **2016**, *2*, 169–174. [CrossRef]
11. Raciti, D.; Livi, K.J.; Wang, C. Highly dense Cu nanowires for low-overpotential CO_2 reduction. *Nano Lett.* **2015**, *15*, 6829–6835. [CrossRef] [PubMed]
12. Cao, L.; Raciti, D.; Li, C.; Livi, K.J.T.; Rottmann, P.F.; Hemker, K.J.; Mueller, T.; Wang, C. Mechanistic insights for low-overpotential electroreduction of CO_2 to CO on copper nanowires. *ACS Catal.* **2017**, *7*, 8578–8587. [CrossRef]
13. Li, J.; Chang, K.; Zhang, H.; He, M.; Goddard, W.A.; Chen, J.G.; Cheng, M.-J.; Lu, Q. Effectively increased efficiency for electroreduction of carbon monoxide using supported polycrystalline copper powder electrocatalysts. *ACS Catal.* **2019**, *9*, 4709–4718. [CrossRef]
14. Hori, Y.; Takahashi, I.; Koga, O.; Hoshi, N. Electrochemical reduction of carbon dioxide at various series of copper single crystal electrodes. *J. Mol. Catal. A Chem.* **2003**, *199*, 39–47. [CrossRef]
15. Hori, Y.; Takahashi, I.; Koga, O.; Hoshi, N. Selective formation of C2 compounds from electrochemical reduction of CO_2 at a series of copper single crystal electrodes. *J. Phys. Chem. B* **2001**, *106*, 15–17. [CrossRef]
16. Perez-Gallent, E.; Marcandalli, G.; Figueiredo, M.C.; Calle-Vallejo, F.; Koper, M.T.M. Structure- and potential-dependent cation effects on CO reduction at copper single-crystal electrodes. *J. Am. Chem. Soc.* **2017**, *139*, 16412–16419. [CrossRef] [PubMed]
17. Ludwig, T.; Gauthier, J.A.; Dickens, C.F.; Brown, K.S.; Ringe, S.; Chan, K.; Nørskov, J.K. Atomistic insight into cation effects on binding energies in Cu-catalyzed carbon dioxide reduction. *J. Phys. Chem. C* **2020**, *124*, 24765–24775. [CrossRef]

18. Murata, A.; Hori, Y. Product selectivity affected by cationic species in electrochemical reduction of CO_2 and CO at a Cu electrode. *Bull. Chem. Soc. Jpn.* **1991**, *64*, 123–127. [CrossRef]
19. Singh, M.R.; Kwon, Y.; Lum, Y.; Ager, J.W., 3rd; Bell, A.T. Hydrolysis of electrolyte cations enhances the electrochemical reduction of CO_2 over Ag and Cu. *J. Am. Chem. Soc.* **2016**, *138*, 13006–13012. [CrossRef]
20. Paik, W.; Andersen, T.N.; Eyring, H. Kinetic studies of the electrolytic reduction of carbon dioxide on the mercury electrode. *Electrochim. Acta* **1969**, *14*, 1217–1232. [CrossRef]
21. Frumkin, A.N. Influence of cation adsorption on the kinetics of electrode processes. *Trans. Faraday Soc.* **1959**, *55*, 156–167. [CrossRef]
22. Thorson, M.R.; Siil, K.I.; Kenis, P.J.A. Effect of cations on the electrochemical conversion of CO_2 to CO. *J. Electrochem. Soc.* **2012**, *160*, F69–F74. [CrossRef]
23. Kaneco, S.; Iiba, K.; Katsumata, H.; Suzuki, T.; Ohta, K. Effect of sodium cation on the electrochemical reduction of CO_2 at a copper electrode in methanol. *J. Solid State Electrochem.* **2006**, *11*, 490–495. [CrossRef]
24. Ringe, S.; Clark, E.L.; Resasco, J.; Walton, A.; Seger, B.; Bell, A.T.; Chan, K. Understanding cation effects in electrochemical CO_2 reduction. *Energy Environ. Sci.* **2019**, *12*, 3001–3014. [CrossRef]
25. Wu, J.; Risalvato, F.G.; Ke, F.-S.; Pellechia, P.J.; Zhou, X.-D. Electrochemical reduction of carbon dioxide I. effects of the electrolyte on the selectivity and activity with Sn electrode. *J. Electrochem. Soc.* **2012**, *159*, F353–F359. [CrossRef]
26. Gao, D.; McCrum, I.T.; Deo, S.; Choi, Y.-W.; Scholten, F.; Wan, W.; Chen, J.G.; Janik, M.J.; Roldan Cuenya, B. Activity and selectivity control in CO_2 electroreduction to multicarbon products over CuOx catalysts via electrolyte design. *ACS Catal.* **2018**, *8*, 10012–10020. [CrossRef]
27. Xi, C.; Zheng, F.; Gao, G.; Ye, M.; Dong, C.; Du, X.-W.; Wang, L.-W. Distribution of alkali cations near the Cu (111) surface in aqueous solution. *J. Mater. Chem. A* **2020**, *8*, 24428–24437. [CrossRef]
28. Ayemoba, O.; Cuesta, A. Spectroscopic evidence of size-dependent buffering of interfacial pH by cation hydrolysis during CO_2 electroreduction. *ACS Appl. Mater. Interfaces* **2017**, *9*, 27377–27382. [CrossRef]
29. Zhang, F.; Co, A.C. Direct evidence of local pH change and the role of alkali cation during CO_2 electroreduction in aqueous media. *Angew Chem. Int. Ed. Engl.* **2020**, *59*, 1674–1681. [CrossRef]
30. Karthik, P.E.; Jothi, V.R.; Pitchaimuthu, S.; Yi, S.; Anantharaj, S. Alternating current techniques for a better understanding of photoelectrocatalysts. *ACS Catal.* **2021**, *11*, 12763–12776. [CrossRef]
31. Sacco, A. Electrochemical impedance spectroscopy as a tool to investigate the electroreduction of carbon dioxide: A short review. *J. CO_2 Util.* **2018**, *27*, 22–31. [CrossRef]
32. Köleli, F.; Röpke, T.; Hamann, C.H. Electrochemical impedance spectroscopic investigation of CO_2 reduction on polyaniline in methanol. *Electrochim. Acta* **2003**, *48*, 1595–1601. [CrossRef]
33. Yang, D.-w.; Li, Q.-y.; Shen, F.-x.; Wang, Q.; Li, L.; Song, N.; Dai, Y.-n.; Shi, J. Electrochemical impedance studies of CO_2 reduction in ionic liquid/organic solvent electrolyte on Au electrode. *Electrochim. Acta* **2016**, *189*, 32–37. [CrossRef]
34. Bienen, F.; Kopljar, D.; Löwe, A.; Geiger, S.; Wagner, N.; Klemm, E.; Friedrich, K.A. Revealing mechanistic processes in gas-diffusion electrodes during CO_2 reduction via impedance spectroscopy. *ACS Sustain. Chem. Eng.* **2020**, *8*, 13759–13768. [CrossRef]
35. Sartori, A.; Orlandi, M.; Berardi, S.; Mazzi, A.; Bazzanella, N.; Caramori, S.; Boaretto, R.; Natali, M.; Fernandes, R.; Patel, N.; et al. Functionalized p-silicon photocathodes for solar fuels applications: Insights from electrochemical impedance spectroscopy. *Electrochim. Acta* **2018**, *271*, 472–480. [CrossRef]
36. Bienen, F.; Kopljar, D.; Geiger, S.; Wagner, N.; Friedrich, K.A. Investigation of CO_2 electrolysis on tin foil by electrochemical impedance spectroscopy. *ACS Sustain. Chem. Eng.* **2020**, *8*, 5192–5199. [CrossRef]
37. Marcandalli, G.; Goyal, A.; Koper, M.T.M. Electrolyte effects on the faradaic efficiency of CO_2 reduction to CO on a gold electrode. *ACS Catal.* **2021**, *11*, 4936–4945. [CrossRef]
38. Zhang, B.A.; Ozel, T.; Elias, J.S.; Costentin, C.; Nocera, D.G. Interplay of homogeneous reactions, mass transport, and kinetics in determining selectivity of the reduction of CO_2 on gold electrodes. *ACS Cent. Sci.* **2019**, *5*, 1097–1105. [CrossRef]
39. Lim, C.F.C.; Harrington, D.A.; Marshall, A.T. Effects of mass transfer on the electrocatalytic CO_2 reduction on Cu. *Electrochim. Acta* **2017**, *238*, 56–63. [CrossRef]
40. Goyal, A.; Koper, M.T.M. The interrelated effect of cations and electrolyte pH on the hydrogen evolution reaction on gold electrodes in alkaline media. *Angew Chem. Int. Ed. Engl.* **2021**, *60*, 13452–13462. [CrossRef]
41. Gupta, N.; Gattrell, M.; MacDougall, B. Calculation for the cathode surface concentrations in the electrochemical reduction of CO_2 in $KHCO_3$ solutions. *J. Appl. Electrochem.* **2005**, *36*, 161–172. [CrossRef]
42. Singh, M.R.; Clark, E.L.; Bell, A.T. Effects of electrolyte, catalyst, and membrane composition and operating conditions on the performance of solar-driven electrochemical reduction of carbon dioxide. *Phys. Chem. Chem. Phys.* **2015**, *17*, 18924–18936. [CrossRef]
43. Kas, R.; Kortlever, R.; Yılmaz, H.; Koper, M.T.M.; Mul, G. Manipulating the hydrocarbon selectivity of copper nanoparticles in CO_2 electroreduction by process conditions. *ChemElectroChem* **2015**, *2*, 354–358. [CrossRef]
44. Bohra, D.; Chaudhry, J.H.; Burdyny, T.; Pidko, E.A.; Smith, W.A. Modeling the electrical double layer to understand the reaction environment in a CO_2 electrocatalytic system. *Energy Environ. Sci.* **2019**, *12*, 3380–3389. [CrossRef]
45. Hori, Y.; Murata, A.; Takahashi, R. Formation of hydrocarbons in the electrochemical reduction of carbon dioxide at a copper electrode in aqueous solution. *J. Chem. Soc. Faraday Trans. 1* **1989**, *85*, 2309–2326. [CrossRef]

46. Dunwell, M.; Yang, X.; Setzler, B.P.; Anibal, J.; Yan, Y.; Xu, B. Examination of near-electrode concentration gradients and kinetic impacts on the electrochemical reduction of CO_2 using surface-enhanced infrared spectroscopy. *ACS Catal.* **2018**, *8*, 3999–4008. [CrossRef]

47. Liu, H.; Liu, J.; Yang, B. Promotional role of a cation intermediate complex in C2 formation from electrochemical reduction of CO_2 over Cu. *ACS Catal.* **2021**, *11*, 12336–12343. [CrossRef]

48. Monteiro, M.C.O.; Dattila, F.; Hagedoorn, B.; García-Muelas, R.; López, N.; Koper, M.T.M. Absence of CO_2 electroreduction on copper, gold and silver electrodes without metal cations in solution. *Nat. Catal.* **2021**, *4*, 654–662. [CrossRef]